*Progress In Electromagnetics Research C, Vol. 138, 27–37, 2023*

# Design of a Compact Dual Slot Loaded Planar Monopole Antenna with Dual Band Rejection Properties for Wideband Applications

**Mattaparthi Nirmala[1, *] and Nagumalli D. Rani[2]**

**Abstract**—This paper presents a novel design of Compact Notched Wide Band Antenna that has dual notches in the band of Wireless Local Area Network (5.15 GHz–5.825 GHz) and X-band Satellite Communication (8 GHz–12 GHz). The proposed antenna has a defective ground structure (DGS) to operate the antenna for wideband applications. Notch bands are achieved by inserting slots on the radiating patch and feed line. A horizontal S-shaped slot on patch is responsible for the notch in the band of wireless local area network, and an inverted U slot is used in feed line to get a notch in the band of Satellite Communication. The proposed antenna is fabricated using an FR4 substrate of size $26 \times 26 \times 1.6\,\text{mm}^3$ and tested using Vector Network Analyzer MS2037C. Although the measured results are slightly changed in comparison with simulated, they agree reasonably well. The measured result also reveals that the prototype antenna is in compact size and resonated from 4.24 GHz–12.59 GHz with two notch bands centered at 5.8 GHz and 10.3 GHz.

## 1. INTRODUCTION

The Federal Communications Commission (FCC) has allocated an unlicensed band that ranges from 3.1 to 10.6 GHz that produces a low equivalent isotropically radiated power (EIRP) of −41.3 dBm [1]. Wideband (WB) antennas are used for communication systems because to their flexible integration with other microstrip circuits, wide impedance bandwidth, cheap cost, light weight, simplicity of manufacture, and low profile. However, other narrowband systems such as IEEE 802.11a WLAN (5.15 GHz–5.35 GHz, 5.725 GHz–5.825 GHz) and X-Band Satellite communication (8 GHz–12 GHz) generally affect WB system in terms of signal interference [2]. A ultra-wideband (UWB) radiator is etched on a Rogers RT5880 substrate with a size of $29 \times 35 \times 0.764\,\text{mm}^3$, operating over a spectrum of 2.66–14.86 GHz with a fractional bandwidth (FBW) of 139%. Dual notched bands at WiMAX (3.01–3.63 GHz) and WLAN (4.48–5.85 GHz) are obtained by etching L-shaped stubs on radiating patch [3]. By presenting a pair of C-shaped parasitic elements and a complementary capacitively loaded loop (CCLL) slot in the ground plane, dual notched bands are accomplished for WLAN band (4.9–6 GHz) and IEEE INSAT C-band/X-band (6.725–7.1 and 7.25–8.4 GHz) satellite services with a gain of 2.7 dBi [4]. Crescent-shaped nested rings are used as both a radiation element and a band rejection element on the radiating patch side. Dual band notch characteristics are obtained in the range 3.15 GHz–3.66 GHz and 4.9 GHz–5.9 GHz [5]. A microstrip-fed antenna is composed of a flared metal plate, a truncated ground plane, and two pairs of folded strips is discussed [6] to get the bandwidth tuning ability at the notched bands. A tapered line resonator is positioned on the radiating patch side to improve group delay response in the notch band [7]. A novel compact UWB multiple-input multiple-output (MIMO) antenna with band rejection is discussed, and the notched band at WLAN (5.15 GHz–5.825 GHz) can be realized by etching a bent

*Received 5 June 2023, Accepted 2 September 2023, Scheduled 25 September 2023*

* Corresponding author: Mattaparthi Nirmala (nirmala.mattaparthi@gmail.com).

[1] Department of ECE, Anil Neerukonda Institute of Technology and Sciences (Autonomous), Visakhapatnam-531162, Andhrapradesh, India. [2] Department of ECE, Gayatri Vidya Parishad College of Engineering (Autonomous), Visakhapatnam-530048, Andhrapradesh, India.

slit in each of the radiating elements [8]. To achieve the dual-frequency rejection of the WLAN at 5.25 GHz and 5.775 GHz bands, double open-circuited stubs are used [9].

It is essential to switch between the various frequency bands to prevent interference. Connecting filters to the WB RF front end to block unused frequency bands is a typical solution to this problem. However, this method may occupy too much space and result in a significant increase in the complexity of the outline. To reduce interference, a possible method is to employ band notching in UWB antennas. However, unlike typical RF filtering techniques, constructing and identifying these notch-creating structures is difficult. A half-wavelength structure, such as a U-shaped slot, C-shaped slot, or an arched slot is typically integrated in the reported antennas [10, 11]. Octagonal patch size of 40 mm × 29 mm is designed to get UWB from 2.70 GHz to 11.06 GHz. Specifically, an L-shaped stub, an inverted C-shaped slot, and a pair of U-shaped resonating structures are introduced into the design, which allow antenna to generate three band notches at 3.22–3.83 GHz, 4.49–5.05 GHz, and 7.49–8.02 GHz, corresponding to WiMAX band and Indian National Satellite (INSAT) band [12]. On the two C-shaped arms and the slots of the rectangular patch, pin diodes are utilized. In the three frequency bands of 3.2–3.75 GHz (WiMAX), 5.05–5.9 GHz (WLAN), and 8–8.45 GHz (ITU), both pin diode modes provide frequency band rejection [13]. A shorted T-shaped quarter-wavelength resonator is utilized first to reject the unwanted 5.1 GHz–5.9 GHz frequency range. Two L-shaped slots are put into the patch to serve as a filter structure for wireless local area network (5 GHz–5.6 GHz) and microwave access (3.4 GHz–3.6 GHz) applications [14]. A modified monopole structure is integrated with an arc-shaped slot and two open-ended L-shaped stubs to realize the band rejection [15]. Furthermore, researchers have used a variety of techniques to achieve super wide bandwidth, including defected ground structures with tapered shape and rectangular slots. DGS is used to improve the gain and bandwidth of microstrip antennas [16]. For attaining band-notch features in WB antennas, several design strategies have been proposed, such as parasitic element loading using fractals, embedding split-ring resonators (SRRs), and electromagnetic band gap (EBG) structures. Different approaches, such as double open-circuited stubs, folded strips, inductive coupling, and half wavelength short-ended split-ring slot, have been used to generate higher-order notch bands. By etching two identical square complementary split ring resonators (CSRRs) in the radiation patch, dual band rejections in the WiMAX and WLAN bands are achieved [17–19]. Dual-band rejection at 4.17–5.33 GHz and 6.5–8.9 GHz in the UWB frequency range by adding three metamaterial (MTM) square split-ring resonators (MTM-SSRRs) and a triangular slot to the radiating patch (3–12 GHz) is discussed. The upper band resonant frequency is controlled by varying the width of the triangular slot width [20]. Novel design of TM-mode dielectric filter is used to generate dual band rejection characteristics in C-band [21]. A compact novel ultra-wideband is designed using a T-shaped slot on radiating patch and partial ground which maintains the peak gain of 3 dB over the passband. Two notch bands are observed at 3.0 to 3.65 GHz and 4.5 to 6.65 GHz, to reject WiMAX and WLAN bands to minimize the effect of interference [22].

In this work, the proposed antenna is designed to cover a wideband range from 4.24 GHz to 12.59 GHz with $S_{11}(\text{dB}) < -10\,\text{dB}$ and VSWR $< 2$ by using defective ground technique (DGS). Narrow band systems like WLAN (5.15 GHz–5.825 GHz), X-band Satellite Communication (8 GHz–12 GHz) are also operating in the wideband range which causes the interference between narrow band systems in WB range. The overall antenna system has compact dimensions of $26 \times 26 \times 1.6\,\text{mm}^3$ compared to the cited work. And this antenna has narrow band systems notching features which are accomplished by inserting a horizontal S-shaped slot on the radiating patch and an inverted U-slot in the feed line structure to prevent interference at WLAN and Point to Point Satellite Communication. The novelty of this proposed antenna is compact size with notch band at X-band satellite applications.

## 2. DUAL BAND NOTCHED WB ANTENNA DESIGN & ANALYSIS

A wideband monopole antenna with a dual band notch is discussed in this research paper. A unique wideband antenna configuration is developed and investigated in terms of $S_{11}$ (dB), voltage standing wave ratio (VSWR), and radiation pattern. The notch bands in the required antenna are accomplished by utilizing an inverted U-slot in the feeding line and a horizontal S-slot in the radiating patch, respectively. The proposed dual band notched WB antenna is designed using an FR4 Epoxy substrate with dielectric constant of 4.4, loss tangent of 0.02, and height 1.6 mm, and is presented in Fig. 1.

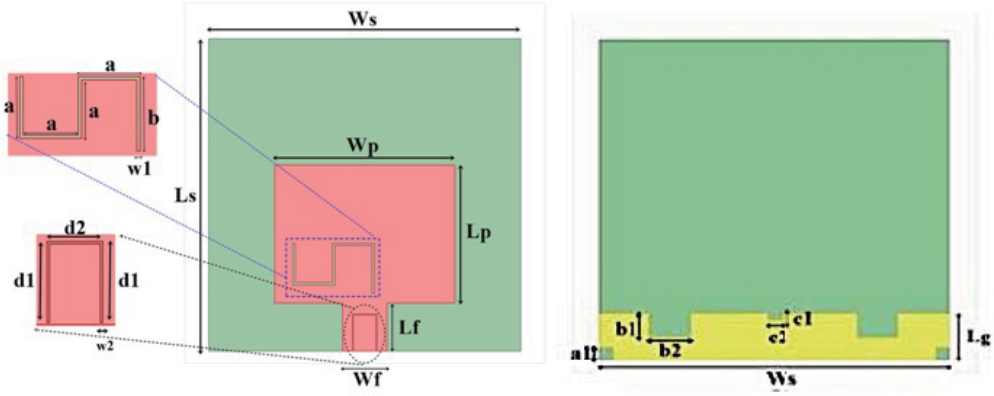


**Figure 1.** Proposed dual band notched WB antenna layout front and back view.

A horizontal S-shaped slot is inserted on the radiating patch to reject WLAN band 5.6 GHz–6.1 GHz centered at 5.8 GHz. An inverted U-slot in the feeding line structure is inserted to get the second band rejection at X-band 9.9 GHz–11 GHz centered at 10.3 GHz. The wideband antenna's operational bandwidth has two notch bands at WLAN and X-band.

## 2.1. WIDE BAND ANTENNA

The wideband antenna is presented in Fig. 2. A basic microstrip patch antenna is designed to resonate at 5.8 GHz frequency [23] using an FR4 Epoxy substrate with dielectric constant of 4.4, loss tangent of 0.02, and height of 1.6 mm. Then basic microstrip patch antenna ground is modified to resonate for a wide range of frequencies of (4.18 GHz–13.38 GHz), which has an impedance bandwidth of 9.2 GHz.

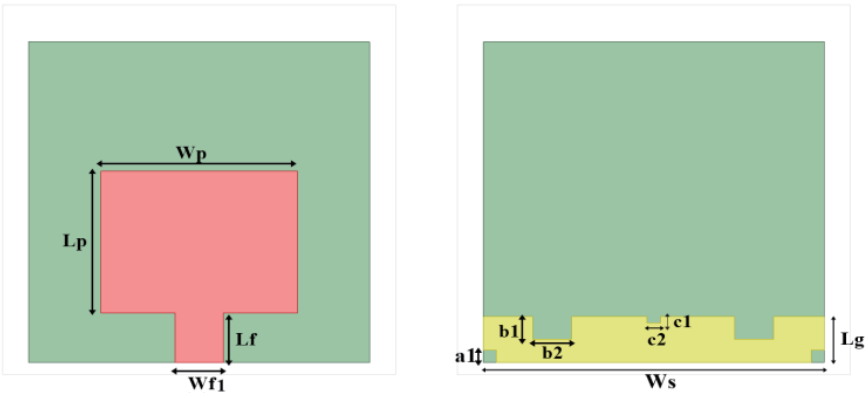


**Figure 2.** Wide band antenna. (a) Front. (b) Back view.

The wideband antenna is designed by using a partial ground $Lg$ and notch depth $b1$. Partial ground reduces the energy stored in the substrate. As the stored energy decreases, Q-factor decreases which in turn increases the bandwidth. Q-factor and bandwidth are inversely proportional as shown in Equation (1).

$$Q = \frac{f_r}{BW} \tag{1}$$

where $fr$ is the resonant frequency, $Q$ the quality factor, and $BW$ the operating bandwidth.

A parametric analysis is carried out in HFSS simulator to get wider bandwidths. Simulations are carried to find the optimized ground length by varying $Lg$ from 3.7 mm to 5.8 mm in steps of 0.7 mm and to find the optimized notch depth by varying $b1$ from 1.6 mm to 1.9 mm in steps of 0.1 mm. The parametric analysis result with respect to ground length ($Lg$) is shown in Fig. 3(a), and that with respect to notch depth ($b1$) is shown in Fig. 3(b).

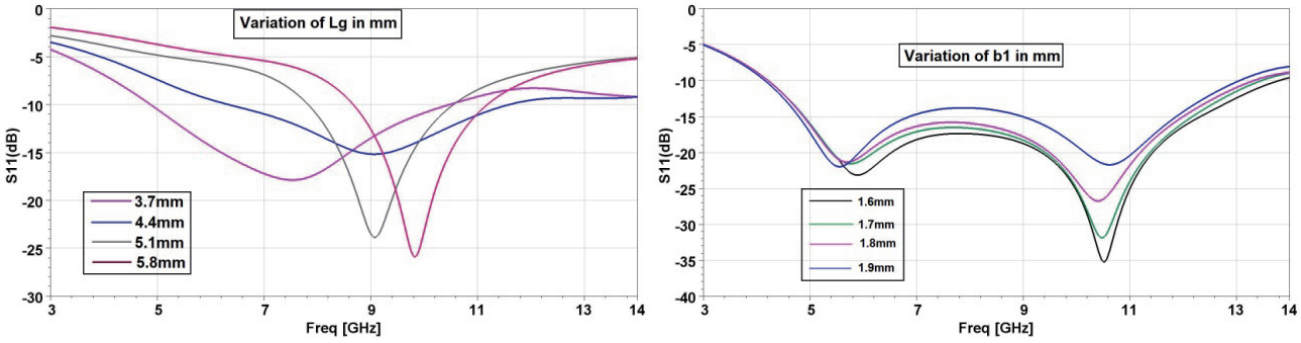


(a) (b)

**Figure 3.** Parametric results. (a) $Lg$ variation, (b) $b1$ variation.

From the parametric analysis results shown in Fig. 3(a), the impedance bandwidth is 5.59 GHz when the ground length is $Lg = 3.7$ mm. The reflection coefficient is below $-10$ dB from 4.86 GHz to 10.44 GHz spectrum. Hence by taking ground length as 3.7 mm, notches are created on partial ground as shown in Fig. 2(b). Parametric analysis is applied to the depth of the notch parameter $b1$. Fig. 3(b) depicts how reflection coefficient is affected by the notch depth $b1$. When notch depth $b1$ is 1.6 mm, the reflection coefficient is below $-10$ dB from 4.22 GHz to 13.78 GHz spectrum. By proper choosing of other dimensions $a1$, $b2$, $c1$, & $c2$, a wideband response is obtained, and it is shown in Fig. 4. The optimized dimension of the WB is listed in Table 1, and the simulation results are shown in Fig. 4.

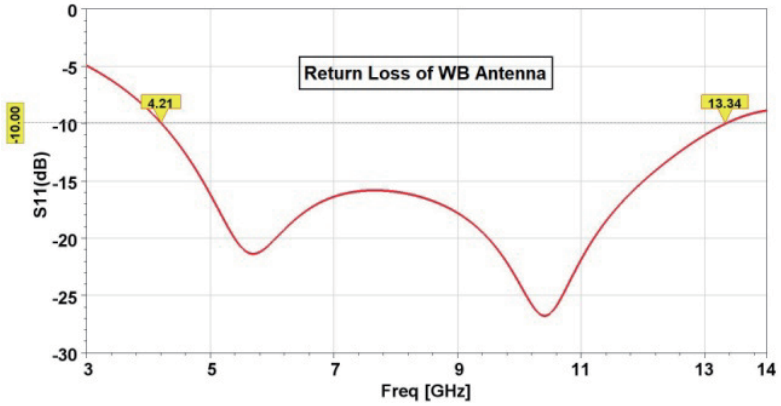


**Figure 4.** WB antenna simulated return loss.

From the simulated return loss shown in Fig. 4, the WB antenna is operating in the frequency range 4.21 GHz–13.34 GHz as $S_{11}$ (dB) is $< -10$ dB.

## 2.2. Single Notch Wide Band Antenna

In order to reject the WLAN frequency range of 5.55 GHz–6.03 GHz, a single band notched WB antenna is designed from wideband antenna. Fig. 5 represents the top view of wideband antenna with single band

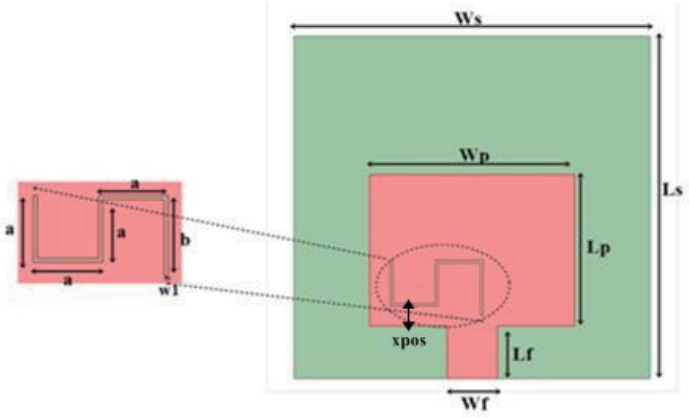


**Figure 5.** Single band notched WB antenna.

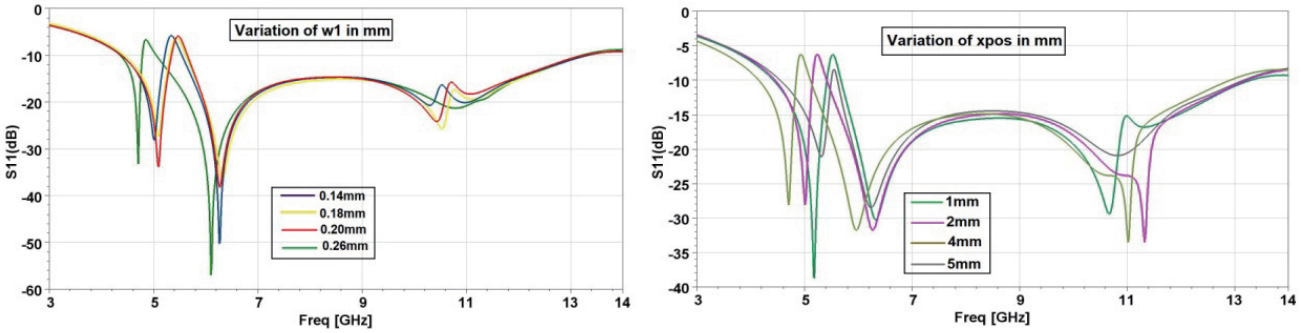


(a) (b)

**Figure 6.** Effect of (a) slot width ($w1$), (b) slot position ($xpos$).

rejection at WLAN frequency range by inserting a horizontal S-shaped slot on patch while maintaining the ground structure as shown in Fig. 2(b).

A horizontal S-shaped slot is inserted on the radiating patch to reject WLAN band. The length of slot is calculated using following Equations (2) and (3).

$$f_r = c/2L\sqrt{\in}_{eff} \tag{2}$$

$$\in_{eff} = \frac{(\in_r +1)}{2} \tag{3}$$

where $f_r$ is the center frequency of notch band, C the speed of light in free space, $\varepsilon_{eff}$ the effective dielectric constant, and $L$ the length of the slot. The length of the slot is taken as $4a + b$ which determines the notch frequency, and the width of the slot determines the bandwidth of the slot. A parametric analysis is carried out to observe the effect of slot width and position on band rejection frequency, and the results are shown in Fig. 6.

Figure 6(a) represents the parametric analysis of slot width $w1$ varying from 0.14 mm to 0.26 mm. When the slot width is at 0.14 mm and 0.26 mm, the notch centre frequency is shifted to lower bands slightly. When $w1$ is 0.20 mm and 0.18 mm, the notch centre frequency is at 5.46 GHz with spectrum from 5.34 GHz to 5.64 GHz. $S_{11}(\text{dB}) = -5.7$ dB when $w1$ is 0.2 mm and $S_{11}(\text{dB}) = -6.3$ dB when $w1$ is 0.18 mm. Hence, $w1 = 0.2$ mm is considered as the optimized slot width. By keeping slot width $w1$ constant, the slot position ($xpos$) is varied with respect to vertical direction. From the parametric results shown in Fig. 6(b), the slot position from 1 mm to 4 mm increases the notch frequency range and return loss at centre frequency. At $xpos$ of 1 mm, the band rejection results in the band 5.40 GHz–5.67 GHz with $S_{11}(\text{dB}) = -5.55$ dB. The optimized dimensions of the horizontal S-shaped slot are mentioned in Table 1.

From the simulated return loss of single band notched WB antenna shown in Fig. 7, the antenna resonates from 4.77 GHz to 13.31 GHz with notch band in the range of 5.67 GHz–5.97 GHz. The centre frequency of notch band is 5.8 GHz with $S_{11}$(dB) of −5.59 dB. The surface current distributions at passband frequency 7.3 GHz and stopband frequency 5.8 GHz are shown in Fig. 8. It can be observed that at passband frequency of 7.3 GHz, the current is totally distributed in the ground and patch except at slot position, but at stopband frequency of 5.8 GHz, the current is totally concentrated around the horizontal S-shaped slot on the radiating patch.

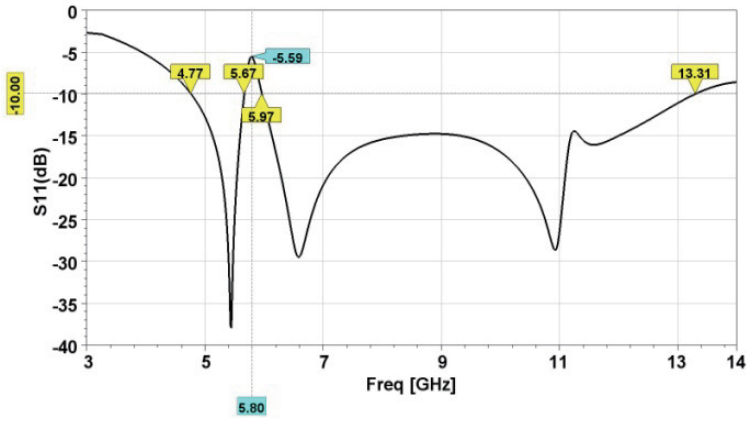


**Figure 7.** Single band notched WB antenna simulated return loss.

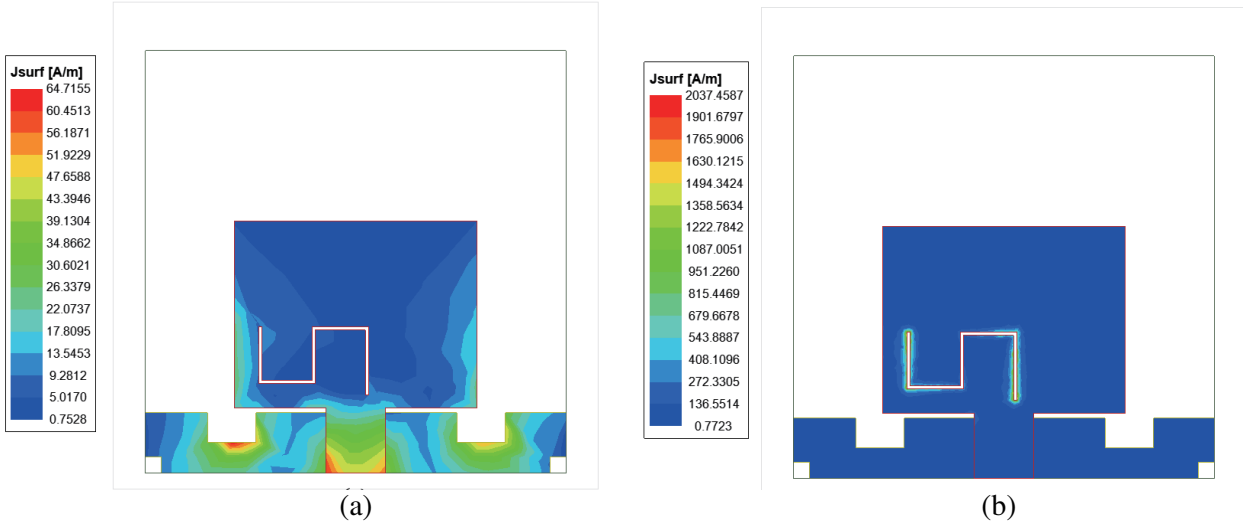


(a) (b)

**Figure 8.** Surface current distribution. (a) Passband frequency of 7.3 GHz. (b) Stopband frequency of 5.8 GHz.

### 2.3. Dual Notch Wide Band Antenna

A single band notched wideband antenna is further designed to reject X-band point to point satellite communication frequency range of 9.81 GHz–11.01 GHz. An inverted U-slot in the feeding line structure is inserted to get the second band rejection at X-band. A dual notch wideband antenna is shown in Fig. 9. An inverted U-slot in the feeding line structure is created with the slot length of $2d1 + d2$. In addition, the width of slot $w2$ and position of the slot have a significant effect on notch band frequency. A parametric analysis is carried out to observe the effect of slot width and position on the notch range and centre frequency, and the results are shown in Fig. 10.

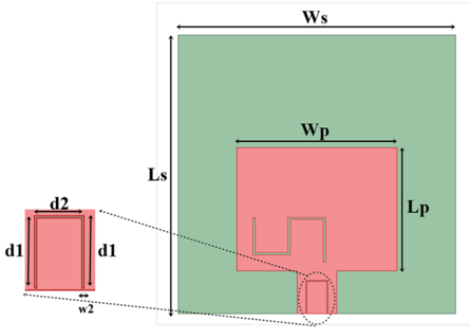


**Figure 9.** Dual band notched WB antenna.

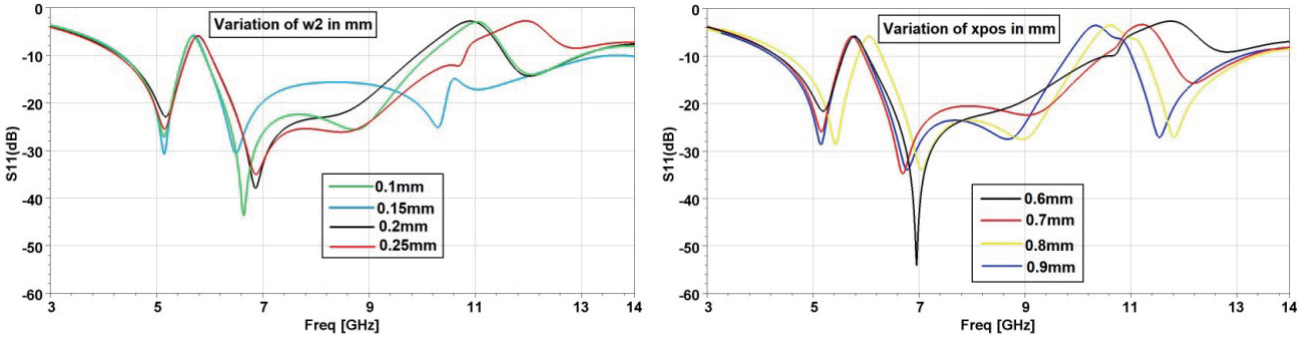


(a) (b)

**Figure 10.** Effect of (a) slot width, (b) slot position.

From the simulated results shown in Fig. 10(a), the slot width $w2$ varies from 0.1 mm to 0.25 mm. When the slot width $w2$ is at 0.2 mm, and notch band occurs from 9.8 GHz to 11.56 GHz. When $w2$ is 0.1 mm, a considerable notch band is observed with the notch centre frequency 10.89 GHz with $S_{11}(\text{dB}) = -3.09$ dB and frequency spectrum of 10.13 GHz–11.46 GHz. Hence, $w2 = 0.1$ mm is considered as optimized value, and keeping width $w2$ constant, the slot position is varied with respect to vertical direction. In Fig. 10(b), slot position is varied from 0.6 mm to 0.9 mm to observe the notch frequency band and $S_{11}$ (dB) at centre frequency. The slot position is considered at 0.9 mm as it results in band notch at X-band (9.8 GHz–11 GHz) with $S_{11}$ (dB) $= -3.33$ dB. The optimized dimensions of inverted U-shaped slot are shown in Table 1.

**Table 1.** Optimized dimensions of proposed antenna.

| **Parameter** | **Ls** | **Ws** | **Lp** | **Wp** | **Lf** | **Wf** | **Wf1** | **Lg** | **b1** | **W2** |
|---|---|---|---|---|---|---|---|---|---|---|
| VALUE (mm) | 26 | 26 | 11.5 | 15.5 | 4 | 1 | 3.65 | 3.7 | 1.8 | 0.1 |
| Parameter | $b2$ | $a1$ | $c1$ | $c2$ | $a$ | $b$ | $w1$ | $d1$ | $d2$ | |
| VALUE (mm) | 3 | 1 | 0.5 | 1 | 3.5 | 4.2 | 0.2 | 3 | 2 | |

## 3. RESULTS AND DISCUSSION

A dual band notch wideband antenna is designed with optimized dimensions and simulated in HFSS. A prototype was then fabricated using an FR4 substrate and tested. Fig. 11 shows the fabricated dual band notched wideband antenna. Measurement results are carried out using Vector Network Analyzer

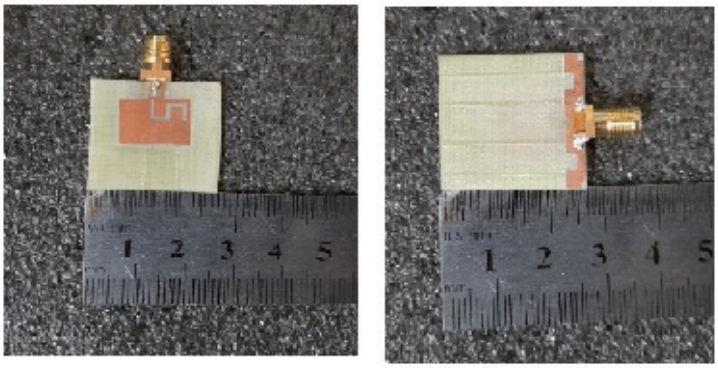


**Figure 11.** Fabricated Prototype of proposed antenna. (a) Front view. (b) Back view.

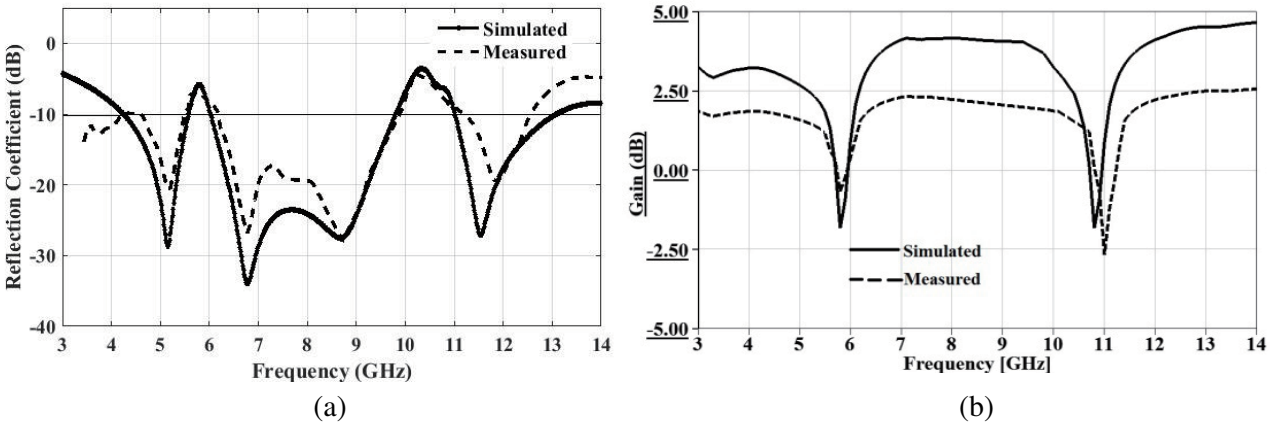


**Figure 12.** Simulated and Measured results. (a) Reflection coefficient. (b) Gain.

MS2037C. Fig. 12(a) indicates that the simulated reflection coefficient is comparable with the measured result in both passband and two stopbands. Fig. 12(b) represents the gain variation with respect to the operating frequency. The minimum gain at notch band is −2.52 dBi, and the maximum gain at pass band is 2.47 dBi. Although the measured results are slightly changed in comparison with simulated ones, they agree reasonably well. The measured result also reveals that the prototype antenna resonates from 4.24 GHz to 12.59 GHz with two notch bands. Lower notch band occurs at WLAN (5.56 GHz–6.03 GHz) with a centre frequency of 5.8 GHz with reflection coefficient of −5.5 dB due to the horizontal S-shaped slot on radiating patch. Upper notch band is developed at X-band (9.8 GHz–11 GHz) with a centre frequency of 10.3 GHz and reflection coefficient of −3.33 dB by inserting an inverted U-slot in the feed line structure. Far field radiation pattern plots in E and H planes at three different frequencies (5 GHz, 8 GHz, & 11.5 GHz) are shown in Fig. 13. In the lower passband at 5 GHz, it is observed that the $E$-plane and $H$-plane show bidirectional characteristics with maximum direction at 0° & 180° with maximum field of 16.5 dB and 18.5 dB, respectively. When the operating frequency is at 8 GHz, the radiation $E$-field pattern shows bidirectional characteristics, but the direction of maxima is slightly shifted by ±15°. The maximum $E$-field values at maxima directions −15° & 195° are 16 dB and 17.45 dB, respectively. A similar pattern in opposite direction maxima is obtained for $H$-field radiation pattern. The maximum $H$-field values at maxima directions 150 & 1650 are 16.2 dB and 17.5 dB, respectively. The third frequency of 11.5 GHz is considered which covers the upper band of operating frequency. It is observed that the $E$-field pattern shows minimum value of −9 dB at −300 and maximum of 14 dB at 1750. The $H$-field pattern is minimum at 300 and maximum at 1950. It can be observed that the simulated radiation patterns are slightly varied with respect to the measured results due to the radiation

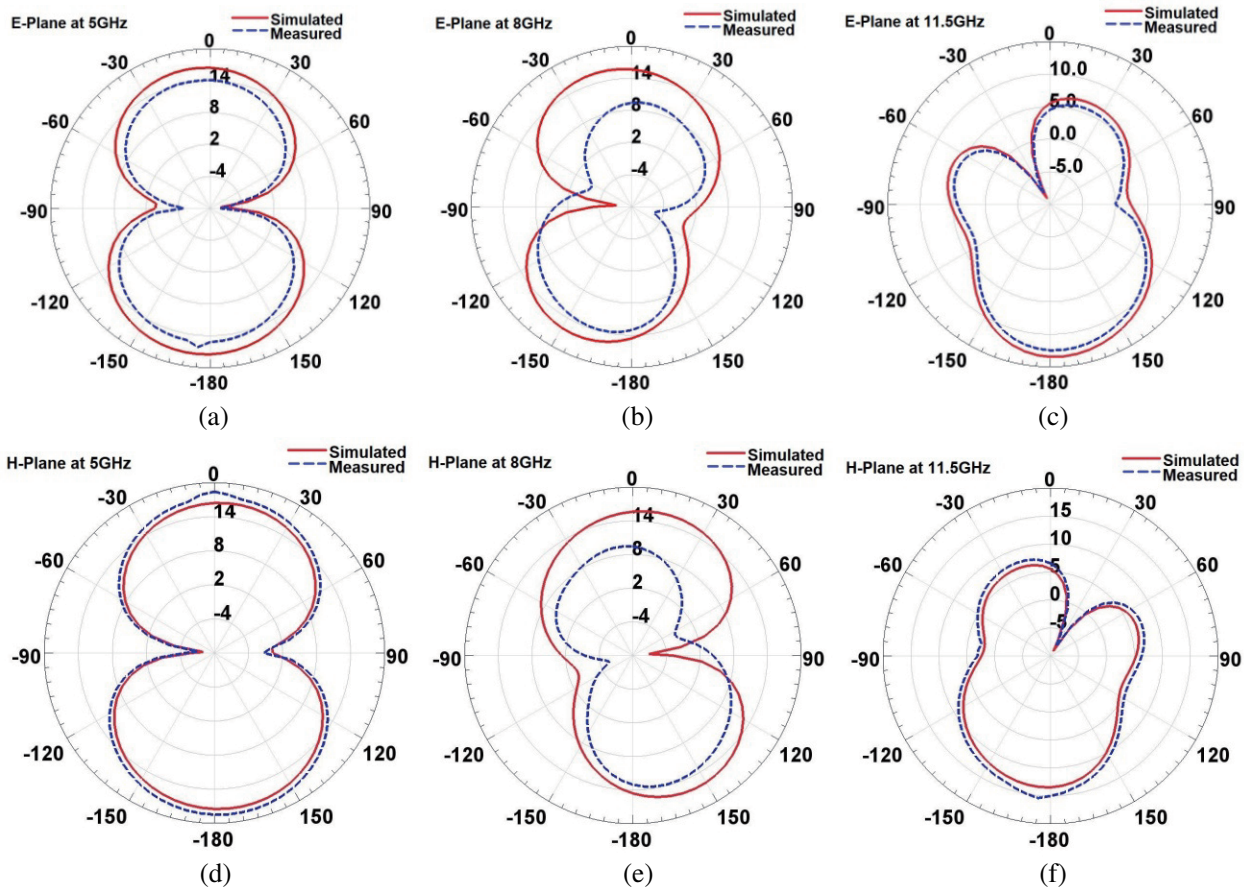


**Figure 13.** Simulated and Measured radiation patterns ($E$ & $H$ planes). (a) $E$-plane at 5 GHz. (b) $H$-plane at 5 GHz. (c) $E$-plane at 8 GHz. (d) $H$-plane at 8 GHz. (e) $E$-plane at 11.5 GHz. (f) $H$-plane at 11.5 GHz.

**Table 2.** Comparison of proposed antenna with reported antennas.

| Reference | Antenna Profile | Notching techniques | Stop Band |
|---|---|---|---|
| Kayhan Celik et al. [5] | $20 \times 30\,\text{mm}^2$ | Parasitic element | Band 1 at 3.41 GHz<br>Band 2 at 5.4 GHz |
| Tzyh et al. [6] | $34 \times 34\,\text{mm}^2$ | Resonator Loaded | 5.3–5.8 GHz |
| Wu et al. [7] | $35 \times 30\,\text{mm}^2$ | Coupled resonator | 4.75–5.95 GHz |
| J.Zhu et al. [8] | $35 \times 35\,\text{mm}^2$ | Etching bent Slits | 5.15–5.82 GHz |
| Gheethan et al. [9] | $44 \times 40\,\text{mm}^2$ | Open circuited stubs | Band 1 at 5.25 GHz<br>Band 2 at 5.775 GHz |
| Nasrabadi et al. [13] | $28 \times 28\,\text{mm}^2$ | Pin diode switching | Band 1 3.2–3.75 GHz<br>Band 2 5.05–5.9 GHz<br>Band 3 8–8.45 GHz |
| Karimian et al. [14] | $14 \times 16\,\text{mm}^2$ | L-shaped slots | Band 1 5–5.6 GHz<br>Band 2 3.4–3.6 GHz |
| Alam et al. [15] | $38 \times 32\,\text{mm}^2$ | Stub/Slots & diodes | Band 1 3.1–4.05 GHz<br>Band 2 5.1–6 GHz |
| This Work | $26 \times 26\,\text{mm}^2$ | Slots on radiating patch | Band 1 5.15–5.825 GHz<br>Band 2 8–12 GHz |

pattern measurement procedure errors.

The measured results of the proposed wideband antenna are compared in Table 2 with some of the reported reconfigurable band rejection UWB antennas. The proposed work is compared with other works in terms of antenna profile size, band rejection technique, and stopband range. Table 2 covers the antenna profile and its notch band characteristics. The antenna profile is same for [5] and proposed antenna, but the substrate material thickness and its dielectric constant are changed. And [5] presents notch bands in lower and middle bands of UWB. The antenna profile size in [6–8] is larger than the proposed work, and single notch band characteristics are presented in the operating band. Dual notch band characteristics are presented in [9, 13, 15] with antenna profile size larger than the proposed work. In [14], the antenna profile size is less than the proposed work, but the dual bands are at different applications. The proposed antenna rejects the X-band applications with low profile size.

## 4. CONCLUSIONS

A dual band notched wideband antenna is proposed and validated in this paper. Wideband antennas are mainly used for military systems requiring multi-functionality. The proposed antenna is designed using FR4 epoxy as substrate to covers a wideband range of 4.24 GHz–12.59 GHz with $S_{11}(\text{dB}) < -10\,\text{dB}$ and VSWR $< 2$ by using defective ground technique (DGS). Narrow band systems like WLAN (5.15 GHz–5.825 GHz) and X-band Satellite Communication (8 GHz–12 GHz) also operate in the wideband range which causes the interference between narrow band systems in WB range. Narrow band systems notching features are accomplished by inserting a horizontal S-shaped slot on the radiating patch and an inverted U-slot in the feed line structure to prevent interference at WLAN and Point to Point Satellite Communication. The overall antenna system has compact dimensions of $26 \times 26 \times 1.6\,\text{mm}^3$. The prototype antenna was fabricated and validated the measured and simulated results for reflection coefficient.

## REFERENCES

1. Federal Communications Commission, "Revision of part 15 of the commission's rules regarding ultra-wideband transmission systems," *First Report and Order, FCC-02*, 2002.
2. Yadav, D., M. P. Abegaonkar, S. K. Koul, et al., "A novel frequency reconfigurable monopole antenna with switchable characteristics between band-notched UWB and WLAN applications," *Progress In Electromagnetics Research C*, Vol. 77, 145–153, 2017.
3. Venkata, S. G. and S. R. K. Kalva, "UWB monopole antenna with dual notched bands verified by characteristic mode analysis (CMA)," *Progress In Electromagnetics Research C*, Vol. 121, 39–48, 2022.
4. Manohar, M., "A High selectivity dual band-stop antenna with wide tuning characteristics for UWB applications," *Analog Integrated Circuits and Signal Processing*, Vol. 111, No. 1, 71–79, 2022.
5. Çelik, K., "A novel circular fractal ring UWB monopole antenna with dual band-notched characteristics," *ETRI Journal*, 2023.
6. Ma, T., R. Hua, and C. Chou, "Design of a multiresonator loaded band-rejected ultrawideband planar monopole antenna with controllable notched bandwidth," *IEEE Transactions on Antennas and Propagation*, Vol. 56, No. 9, 2875–2883, Sept. 2008.
7. Wu, S.-J., C.-H. Kang, K.-H. Chen, C.-K. Chan, and J.-H. Tarng, "A notched-band UWB planar monopole antenna using the tapped-line coupled resonator," *2009 Asia Pacific Microwave Conference, IEEE*, 2486–2489, 2009.
8. Zhu, J., S. Li, B. Feng, L. Deng, and S. Yin, "Compact dual-polarized UWB quasi-self-complementary MIMO/diversity antenna with band-rejection capability," *IEEE Antennas and Wireless Propagation Letters*, Vol. 15, 905–908, 2016.
9. Gheethan, A. and D. E. Anagnostou, "Dual band-reject UWB antenna with sharp rejection of narrow and closely-spaced bands," *IEEE Transactions on Antennas and Propagation*, Vol. 60, No. 4, 2071–2076, April 2012.

10. Sohail, A., K. S. Alimgeer, A. Iftikhar, et. al., "Dual notch band UWB antenna with improved notch characteristics," *Microwave and Optical Technology Letters*, Vol. 60, No. 4, 925–930, 2018.
11. Gujjula, V., M. Nirmala, B. R. M. Krishna, and N. D. Rani, "Design of ultra-wideband antenna with dual notch characteristics at WiMAX/WLAN bands," *2019 IEEE International Conference on Intelligent Systems and Green Technology (ICISGT)*, 28–282, 2019.
12. Lin, H., Z. Lu, Z. Wang, and W. Mu, "A compact UWB monopole antenna with triple band notches," *Micromachines*, Vol. 14, No. 3, 518, 2023.
13. Nasrabadi, E. and P. Rezaei, "A novel design of reconfigurable monopole antenna with switchable triple band-rejection for UWB applications," *International Journal of Microwave and Wireless Technologies*, Vol. 8, No. 8, 1223–1229, 2016.
14. Karimian, R., H. Oraizi, and S. Fakhte, "Design of a compact ultra wideband monopole antenna with band rejection characteristics," *IET Microwaves, Antennas & Propagation*, Vol. 8, No. 8, 604–610, 2014.
15. Alam, M. S. and A. Abbosh, "Reconfigurable band rejection antenna for ultra wideband applications," *IET Microwaves, Antennas & Propagation*, Vol. 12, No. 2, 195–202, 2018.
16. Ullah, S., C. Ruan, M. S. Sadiq, et al., "Super wide band, defected ground structure (DGS), and stepped meander line antenna for WLAN/ISM/WiMAX/UWB and other wireless communication applications," *Sensors*, Vol. 20, No. 6, 1735, 2020.
17. Kumar, G., D. Singh, and R. Kumar, "A planar CPW fed UWB antenna with dual rectangular notch band characteristics incorporating U-slot, SRRs, and EBGs," *International Journal of RF and Microwave Computer Aided Engineering*, Vol. 31, No. 7, e22676, 2021.
18. Lai, H., et al., "UWB antenna with dual band rejection for WLAN/WiMAX bands using CSRRs," *Progress in Electromagnetics Research Letters*, Vol. 26, 69–78, 2011.
19. Iqbal, A., O. A. Saraereh, and S. K. Jaiswal, "Maple leaf shaped UWB monopole antenna with dual band notch functionality," *Progress In Electromagnetics Research C*, Vol. 71, 169–175, 2017.
20. Vallappil, A. K., B. A. Khawaja, M. K. A. Rahim, M. N. Iqbal, H. T. Chattha, and M. F. B. M. Ali, "A compact triple-band UWB inverted triangular antenna with dual-notch band characteristics using SSRR metamaterial structure for use in next-generation wireless systems," *Fractal Fract*, Vol. 6, 422, 2022.
21. Widaa and M. Höft, "Miniaturized dual-band dual-mode TM-mode dielectric filter in planar configuration," *IEEE Journal of Microwaves*, Vol. 2, No. 2, 326–336, April 2022, doi: 10.1109/JMW.2022.3145906.
22. Yadav, A., P. Singh, R. K. Verma, and V. K. Singh, "Design and comparative analysis of circuit theory model-based slot-loaded printed rectangular monopole antenna for UWB applications with notch band," *Int. J. Commun. Syst.*, e5390, 2022.
23. Balanis, C. A., *Antenna Theory: Analysis and Design*, John Wiley & Sons, 2015.